

Variability of PD-L1 expression in mastocytosis

Ellen W. Hatch,^{1,*} Mary Beth Geeze,^{1,*} Cheyenne Martin,¹ Mohamed E. Salama,² Karin Hartmann,³ Gregor Eisenwort,^{4,5} Katharina Blatt,^{4,5} Peter Valent,^{4,5} Jason Gotlib,⁶ Ji-Hyun Lee,⁷ Lu Chen,⁷ Heather H. Ward,^{7,8} Diane S. Lidke,^{1,7} and Tracy I. George^{1,7}

¹Department of Pathology, University of New Mexico, Albuquerque, NM; ²Department of Pathology, University of Utah, Salt Lake City, UT; ³Department of Dermatology, University of Luebeck, Luebeck, Germany; ⁴Division of Hematology and Hemostaseology, Department of Internal Medicine I, and ⁵Ludwig Boltzmann Cluster Oncology, Medical University of Vienna, Vienna, Austria; ⁶Stanford Cancer Institute, School of Medicine, Stanford University, Stanford, CA; and ⁷Comprehensive Cancer Center and ⁸Department of Internal Medicine, University of New Mexico, Albuquerque, NM

Key Points

- PD-L1 is variably expressed in MCs from patients with SM and CM.
- PD-1 is expressed in MCs in a subset of patients with CM, but not SM.

Mastocytosis is a rare disease with heterogeneous clinical manifestations and few effective therapies. Programmed death-1 (PD-1) and its ligands (PD-L1 and PD-L2) protect tissues from immune-mediated damage and permit tumors to evade immune destruction. Therapeutic antibodies against PD-1 and PD-L1 are effective in the treatment of a variety of neoplasms. In the present study, we sought to systematically analyze expression of PD-1 and PD-L1 in a large number of patients with mastocytosis using immunohistochemistry and multiplex fluorescence staining. PD-L1 showed membrane staining of neoplastic mast cells (MCs) in 77% of systemic mastocytosis (SM) cases including 3 of 3 patients with MC leukemia, 2 of 2 with aggressive SM, 1 of 2 with smoldering SM, 3 of 4 with indolent SM, and 9 of 12 with SM with an associated hematologic neoplasm (SM component only). Ninety-two percent (23 of 25) of cutaneous mastocytosis (CM) cases and 1 of 2 with myelomastocytic leukemia expressed PD-L1, with no expression found in 15 healthy/reactive marrows, 18 myelodysplastic syndromes (MDSs), 16 myeloproliferative neoplasms (MPNs), 5 MDS/MPNs, and 3 monoclonal MC activation syndromes. Variable PD-L1 expression was observed between and within samples, with PD-L1 staining of MCs ranging from 10% to 100% (mean, 50%). PD-1 dimly stained 4 of 27 CM cases (15%), with no expression in SM or other neoplasms tested; PD-1 staining of MCs ranged from 20% to 50% (mean, 27%). These results provide support for the expression of PD-L1 in SM and CM, and PD-1 expression in CM. These data support the exploration of agents with anti-PD-L1 activity in patients with advanced mastocytosis.

Introduction

Mastocytosis is a rare disease with heterogeneous clinical manifestations ranging from cutaneous mastocytosis (CM) in pediatric patients, characterized by an indolent course and regression at puberty in a subset of cases, to advanced systemic mastocytosis (SM) in adults with poor prognosis.^{1,2} Advanced SM includes mast cell (MC) leukemia (MCL), aggressive SM (ASM) and SM with an associated hematological neoplasm (SM-AHN). These various categories of mastocytosis have in common activating mutations of *KIT*, in particular D816V, which results in constitutive KIT receptor tyrosine kinase signaling.³ Despite an understanding of the main genetic driver of mastocytosis, few effective therapies are currently available.⁴

Programmed death 1 (PD-1) and its ligands (PD-L1 and PD-L2) are known to protect tissues from immune-mediated damage, but dysregulation of this epitope pair can also allow tumors to evade immune

Submitted 11 August 2017; accepted 29 December 2017. DOI 10.1182/bloodadvances.2017011551.

*E.W.H. and M.B.G. contributed equally to this study.

Presented in part at the annual meeting of the United States and Canadian Academy of Pathology, Seattle, WA, 16 March 2016.

The full-text version of this article contains a data supplement.

© 2018 by The American Society of Hematology

Table 1. Characterization of antibodies

Antigen	CD	Clone	Conjugate	Supplier
HPCA1	CD34	581	Pacific Blue	BioLegend
PTPRC	CD45	HI30	APC/Cy7	BioLegend
KIT	CD117	104D2	PE/Cy	eBioscience
PD-L1	CD274	29E.2A3	PE	BioLegend
PD-1	CD279	EH12.2H7	PE	BioLegend
IgG1 isotype control	n.c.	—	PE	BD Biosciences

—, no clone available; APC, allophycocyanin; Cy7, cyanine 7; HPCA1, human precursor cell antigen 1; Ig, immunoglobulin; n.c., not yet clustered; PE, phycoerythrin; PTPRC, protein tyrosine phosphatase, receptor type C.

cell-mediated targeting and subsequent destruction.⁵ Novel antibodies against PD-1 and PD-L1 have been shown to be effective in a variety of solid tumors.⁶ Recently, levels of soluble PD-L1 in the serum of adult mastocytosis patients were shown to correlate with disease status.⁷ Higher levels of serum PD-L1 have been described in patients with advanced SM compared with indolent SM (ISM). Furthermore, SM and CM patient samples can exhibit PD-1 and PD-L1 protein expression.⁷

Here, we examined the expression of PD-1 and PD-L1 in different tissues of a large number of SM and CM cases, including advanced SM, as well as reactive bone marrows (BMs), BMs involved by myeloproliferative neoplasms (MPNs), myelodysplastic syndrome (MDS), and MDS/MPN, and healthy skin controls. We further sought to confirm MC coexpression of tryptase and PD-L1 and to examine potential variability within samples using flow cytometry and multiplex immunohistofluorescence (IHF) staining.

Materials and methods

Tissue samples

After institutional review board approval, we evaluated 122 paraffin-embedded tissues (BM, skin, spleen, lymph node) from patients with CM, SM, healthy/reactive BM, MDS, MPN, MDS/MPN, myelomastocytic leukemia (MML), and monoclonal MC activation syndrome (MMAS). Samples were taken at diagnosis for all patients; healthy/reactive BMs were typically negative staging marrows for patients with lymphoma. Skin, spleen, and lymph nodes were fixed in 10% neutral-buffered formalin. BM included formalin-fixed/EDTA-decalcified specimens and acetic zinc formalin-fixed/rapid decalcified specimens. Both tissue microarrays and whole section slides were used for immunohistochemistry (IHC). All cases were diagnosed according to the revised criteria of the 2016 World Health Organization (WHO) classification and published criteria for MML.^{8,9} Placenta and tonsil were used as positive labeling controls for PD-L1 and PD-1, respectively. Spleen from 1 patient with MCL and 2 patients with CM were used for multiplex IHF, in addition to appropriate control tissue (healthy skin and spleen). BM aspirate samples for flow cytometry were obtained from the iliac crest of 3 patients with ISM, 1 with ASM, and 2 with MCL. Cells were collected during routine diagnostic investigations. All patients provided written informed consent.

IHC

We evaluated protein expression of PD-1 (MRQ-22; Cell Marque, Rocklin, CA) and PD-L1 (E1L3N; Cell Signaling Technology,

Danvers, MA). IHC was performed with BenchMark Ultra (Ventana Medical Systems, Tucson, AZ) using automated antigen retrieval (CC1 enzyme digestion). Slides were scored by the authors (M.B.G., T.I.G.) on a 0 to 3 scale for staining intensity (0 = no staining; 1 = no tissue; 2 = dim; 3 = strong) and an overall percentage of cells staining positive was recorded.

Flow cytometric evaluation of expression of PD-1 and PD-L1 on MCs

BM mononuclear cells were isolated using Ficoll (Biochrom, Berlin, Germany). BM mononuclear cells were treated with Fc-blocking reagent (Miltenyi Biotec, Bergisch Gladbach, Germany) and stained with the following fluorochrome-labeled monoclonal antibodies (Table 1): CD117-phycoerythrin (PE)/Cy7 (eBioscience), CD34–Pacific Blue, CD45-allophycocyanin/Cy7, CD274-PE, CD279-PE, and mouse immunoglobulin G₁ (IgG₁)–PE (BioLegend). MCs were defined as CD45⁺/CD34[−]/CD117^{hi} cells. Expression of PD-1 (CD279) and PD-L1 (CD274) on MCs was analyzed by multicolor flow cytometry on a FACSCanto II flow cytometer (BD Biosciences). The human MCL-like cell lines HMC-1.1 and HMC-1.2 were kindly provided by Joseph H. Butterfield (Mayo Clinic, Rochester, MN). HMC-1 cells were treated with Fc-blocking reagent and then stained with monoclonal antibodies against CD274 (CD274-PE), CD279 (CD279-PE), and mouse IgG₁-PE, and analyzed on a FACSCalibur (BD Biosciences).

Multicolor IHF

Paraffin-embedded tissue samples were first deparaffinized followed by antigen retrieval using citrate buffer pH 6 in a Biocare Medical DC2002 (Concord, CA) decloaking chamber, which cycled from room temperature up to 120°C for 5 minutes. Tissue was incubated with anti-PD-L1 primary antibody SP142 (1:100; Spring Bioscience, Pleasanton, CA) for 2 hours at room temperature, followed by Alexa Fluor 488–conjugated secondary antibodies (1:200, A11070; Thermo Fisher Scientific) for 2 hours at room temperature. The anti-tryptase antibody (sc59587X; Santa Cruz Biotechnology, Santa Cruz, CA) was directly conjugated to Alexa Fluor 647 (AF647) by reaction of Alexa Fluor 647–N-hydroxysuccinimide ester and carrier-free antibody at a 10:1 molar ratio in phosphate-buffered saline plus sodium carbonate buffer, pH 8.0. Free dye was removed by passing the mixture through a size-exclusion column (PD MiniTrap G-25). Absorbance measurements indicated a final dye-to-protein ratio of 0.92. Anti-tryptase–AF647 and anti-PD-L1 primary antibodies were incubated with the tissue simultaneously. Nuclei were stained with 4',6-diamidino-2-phenylindole, dihydrochloride (DAPI; 100 ng/mL, Sigma, St. Louis, MO) for 5 minutes before final mounting of the tissue with Prolong Gold Antifade Mount (P36930; Thermo Fisher Scientific, Waltham, MA).

Wide-field images were acquired using an epifluorescence microscope (Zeiss AxioPlan2 or Nikon TE2000) equipped with a Nuance Multi-Spectral camera (PerkinElmer, Cambridge, MA) and software (version 3.0.2; PerkinElmer) that allows for spectral unmixing of multicolor images and separation of background autofluorescence. Nikon filters used included DAPI (excitation BP, 330–380 nm; emission LP, 420 nm), Alexa Fluor 488 (fluorescein isothiocyanate) (excitation BP, 465 m to 495 nm; emission LP, 515 nm), and Alexa Fluor 647 (excitation BP, 620/60 nm; emission BA, 700/75 nm); 20× and 60× objectives were used resulting in 0.5 μm per pixel or 0.1654 μm per pixel, respectively. AxioPlan2

Table 2. Clinical, laboratory, and immunohistochemical characteristics of mastocytosis patients

Patient	Age, y	Sex	Biopsy site	Diagnosis	Serum tryptase, ng/ μ L	KIT mutation	PD-1 expression	PD-1 MC, %	PD-L1 expression	PD-L1 MC, %
1	62	F	LN	MCL	NA	D816V ⁺	0	0	NA	NA
2	61	NA	BM	MCL	NA	D816V ⁻	0	0	3	80
3	NA	NA	BM	MCL	NA	NA	0	0	2	50
4	48	F	BM	MCL-MDS/MPN-U	>200	D816V ⁺	0	0	2	50
5	30	F	BM	ASM	NA	D816V ⁻	0	0	2	10
6	NA	NA	BM	ASM	NA	NA	0	0	2	20
7	46	M	BM	SM-CMML-1	NA	D816V ⁻	0	0	3	70
8	72	M	BM	SM-CMML-1	NA	D816V ⁺	0	0	2	50
9	68	F	BM	SM-CMML-1	NA	D816V ⁺	0	0	3	80
10	76	F	BM	SM-CMML-1	NA	D816V ⁺	0	0	3	80
11	NA	NA	BM	SM-CMML-1	NA	NA	0	0	3	50
12	62	M	BM	SM-CMML-1	NA	D816V ⁺	0	0	3	50
13	67	M	BM	SM-CMML-1	NA	D816V ⁺	0	0	2	10
14	79	M	BM	SM-CMML-1	NA	D816V ⁺	0	0	0	0
15	65	M	BM	SM-CMML-1	NA	D816V ⁺	0	0	0	0
16	24	M	BM	SM-MDS/MPN-U	NA	D816V ⁺	0	0	0	0
17	NA	NA	BM	SM-AML	NA	NA	0	0	2	40
18	NA	NA	BM	SM-AML	NA	NA	0	0	NA	NA
19	NA	NA	BM	SM-AHN	NA	NA	0	0	NA	NA
20	NA	NA	BM	SSM	NA	NA	0	0	3	90
21	NA	NA	BM	SSM	NA	NA	0	0	0	0
22	NA	NA	BM	ISM	NA	NA	0	0	2	20
23	NA	NA	BM	ISM	NA	NA	0	0	2	10
24	NA	NA	BM	ISM	NA	NA	0	0	2	50
25	NA	NA	BM	ISM	NA	NA	0	0	0	0
26	NA	NA	BM	MML	NA	NA	0	0	2	10
27	NA	NA	BM	MML	NA	NA	0	0	0	0
28	16	F	Skin, R neck	MPCM	NA	NA	2	30	2	80
29	0.83	F	Skin, chest	MPCM	NA	NA	0	0	0	0
30	0.25	F	Skin, back	MPCM	NA	NA	0	0	3	80
31	24	F	Skin, L back	MPCM	NA	NA	0	0	3	50
32	32	F	Skin, R thigh	MPCM	NA	NA	0	0	3	50
33	0.33	M	Skin, abdomen	MPCM	NA	NA	0	0	0	0
34	39	M	Skin, L forearm	MPCM	NA	NA	NA	NA	NA	NA
35	56	F	Skin, L thigh	MPCM	NA	NA	2	25	NA	NA
36	2	F	Skin, back	MPCM	NA	NA	0	0	2	20

Immunohistochemical expression of PD-1 and PD-L1 is scored as 0 (negative), 2 (dim), and 3 (moderate). The percentage of MCs stained by the antibody is estimated as a percentage out of total MCs present in the biopsy section on the slide.
 AML, acute myeloid leukemia; CMML-1, chronic myelomonocytic leukemia-1; F, female; L, left; LN, lymph node; M, male; MDS/MPN-U, myelodysplastic/myeloproliferative neoplasm, unclassifiable; MIS, mastocytosis in skin; MPCM, maculopapular CM; NA, not available; NOS, not otherwise specified; R, right; SSM, smoldering SM.

Table 2. (continued)

Patient	Age, y	Sex	Biopsy site	Diagnosis	Serum tryptase, ng/μL	KIT mutation	PD-1 expression	PD-1 MC, %	PD-L1 expression	PD-L1 MC, %
37	79	M	Skin, back	MPCM	NA	NA	0	0	2	30
38	61	F	Skin, R calf	MPCM	NA	NA	0	0	3	70
39	17	F	Skin, L anterior forearm	MPCM	NA	NA	0	0	2	20
40	59	M	Skin, L back	MPCM	NA	NA	0	0	2	50
41	51	F	Skin, R upper thigh	MPCM	NA	NA	0	0	3	80
42	8	M	Skin, back	MPCM	NA	NA	0	0	2	20
43	9	M	Skin, L shoulder	MPCM	NA	NA	0	0	3	50
44	49	F	Skin, L breast	MPCM	NA	D816V ⁻	0	0	3	60
45	3	M	Skin, L flank	MPCM	NA	NA	0	0	2	20
46	31	F	Skin, R thigh	MPCM	NA	NA	0	0	3	20
47	1	M	Skin, scalp	Mastocytoma	NA	NA	0	0	2	20
48	1	M	Skin, R forearm	Mastocytoma	NA	NA	2	20	2	50
49	0.17	M	Skin, R side	Mastocytoma	NA	NA	2	20	2	90
50	NA	NA	Skin, NOS	MIS	NA	NA	0	0	3	80
51	NA	NA	Skin, NOS	MIS	NA	NA	0	0	3	90
52	63	F	Skin, R leg	MIS	NA	D816V ⁺	0	0	3	75
53	53	F	Skin, R abdomen/R thigh	MIS	40	NA	0	0	NA	NA
54	22	M	Skin, L wrist	MIS	18.2	NA	0	0	2	30
55	22	M	Skin, L plantar foot	MIS	18.2	NA	0	0	2	30

Immunohistochemical expression of PD-1 and PD-L1 is scored as 0 (negative), 2 (dim), and 3 (moderate). The percentage of MCs stained by the antibody is estimated as a percentage out of total MCs present in the biopsy section on the slide. AML, acute myeloid leukemia; CMML-1, chronic myelomonocytic leukemia-1; F, female; L, left; LN, lymph node; M, male; MDS/MPN-U, myelodysplastic/myeloproliferative neoplasm, unclassifiable; MIS, mastocytosis in skin; MPCM, maculopapular CM; NA, not available; NOS, not otherwise specified; R, right; SSM, smoldering SM.

Table 3. Summary of expression of PD-1 and PD-L1 in mastocytosis subtypes, other myeloid neoplasms, and reactive/healthy BMs using IHC

Diagnosis	PD-L1 expression (%) [*]	PD-1 expression (%) [†]
SM[‡]	17/22 (77)	0/25 (0)
MCL [‡]	3/3 (100)	0/4 (0)
ASM	2/2 (100)	0/2 (0)
SM-AHN [§]	9/12 (75)	0/14 (0)
SSM	1/2 (50)	0/2 (0)
ISM	3/4 (75)	0/4 (0)
CM	23/25 (92)	4/27 (15)
MPCM	15/17 (88)	2/18 (11)
Mastocytoma	3/3 (100)	2/3 (67)
MIS	5/5 (100)	0/6 (0)
MML	1/2 (50)	0/2 (0)
MMAS [§]	0/3 (0)	0/3 (0)
MPN [§]	0/16 (0)	0/17 (0)
MDS [§]	0/18 (0)	0/18 (0)
MDS/MPN [§]	0/5 (0)	0/5 (0)
Healthy and reactive BM [§]	0/15 (0)	0/21 (0)

MDS/MPNs are all chronic myelomonocytic leukemia. MPNs included primary myelofibrosis (3), polycythemia vera (4), essential thrombocythemia (3), chronic myeloid leukemia (4), and chronic eosinophilic leukemia not otherwise specified (3). MDSs included 5q-syndrome (4), MDS with excess blasts (3), MDS with single-lineage dysplasia (i.e., refractory anemia) (1), MDS with multilineage dysplasia (5), MDS with single-lineage dysplasia and ring sideroblasts (4), and MDS not otherwise specified (1). MIS refers to skin lesions of mastocytosis in patients with SM or MCL.

^{*}PD-L1 positivity correlated with expression in SM ($P = .0002$) and CM ($P = .0147$), but did not correlate with subtype of SM or CM ($P =$ not significant).

[†]PD-1 positivity correlated with expression in CM ($P = .0156$) and subtype of CM ($P = .0336$).

[‡]MCL and SM-AHN both include a single patient with MCL-MDS/MPN-U (patient 4 from Table 2). This patient is only included once in the overall total of SM patients.

[§]Immunohistochemical expression of PD-L1 and PD-1 refers to expression in MCs.

filters from Zeiss and Semrock included DAPI (excitation BP, 365/25 nm; emission LP, 420 nm), Alexa Fluor 488 (excitation BP, 485/20 nm; emission LP, 515 nm), and Alexa Fluor 647 (excitation BP, 628/32 nm; emission LP, 665 nm); 20 \times and 63 \times objectives were used resulting in 0.5 μ m per pixel or 0.157 μ m per pixel, respectively.

Confocal images were acquired using a Leica SP8 laser-scanning confocal microscope with a 63 \times 1.4 numerical aperture oil objective, resulting in 0.18 μ m per pixel. Spectral images were collected using spectral scan mode (xyz). Excitation was with 405-nm, 488-nm, and 633-nm laser lines. Emission was collected from 430 nm to 700 nm using a 20-nm band in 10-nm increments. Control spectra for unmixing were acquired from single-labeled control slides. Linear unmixing was performed using LAS X linear software (Leica). Seven regions of interest were tiled together to form a large, high-resolution field of view as seen in Figure 6. All fluorescence images are brightness and contrast enhanced.

Statistics

Statistical analysis was performed using SAS version 9.4 (SAS Institute Inc, Cary, NC). The Kruskal-Wallis test (if numerical covariate) or Pearson χ^2 (if categorical covariate) was used to

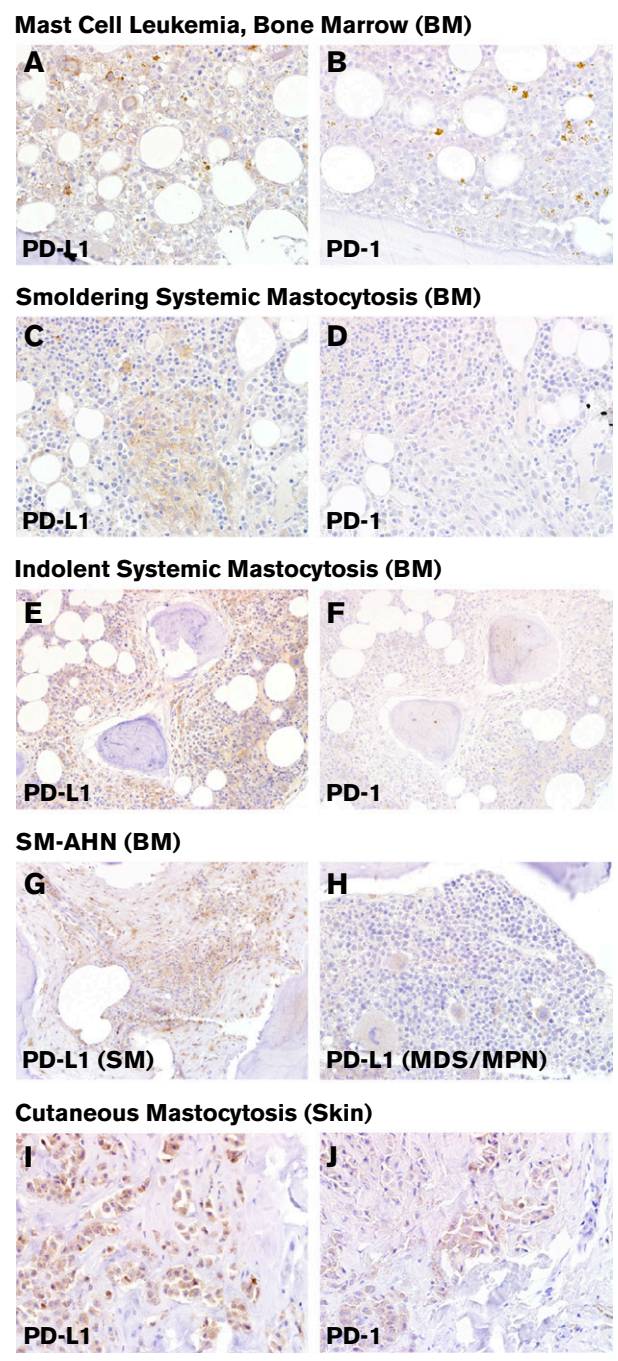


Figure 1. Immunohistochemical staining of PD-L1 and PD-1 in mastocytosis. Immunohistochemical expression of PD-L1 is shown at left for (A) MCL, (C) smoldering SM, (E) ISM, (G) SM-AHN (MDS/MPN), and (I) CM. At right, immunohistochemical staining for PD-1 is shown for (B) MCL, (D) smoldering SM, (F) ISM, and (J) CM. (G-H) In SM-AHN (MDS/MPN), the PD-L1 expression is restricted to the MC component as shown in panel G, but it is not present in the associated hematologic neoplasm as shown in panel H. Magnification $\times 40$ in panels A-D, I-J and $\times 20$ in panel E-H. Images taken with an Olympus BX41 microscope with Olympus cellSens standard version 1.14 software, and standard color balancing and image sizing using Adobe Photoshop.

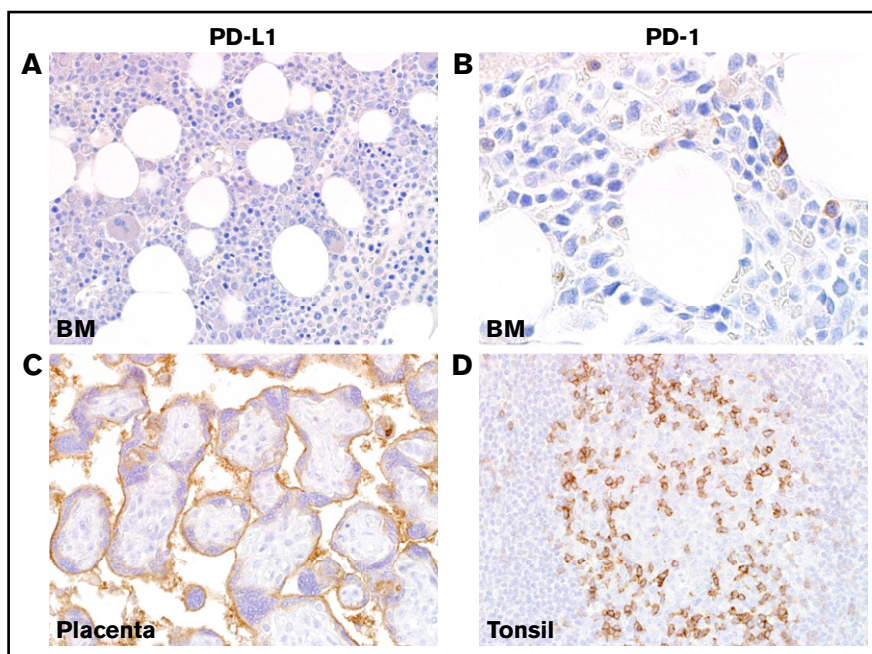


Figure 2. Immunohistochemical staining of PD-L1 and PD-1 in healthy BM and controls. (A) IHC for PD-L1 showed no staining in healthy or reactive BM. (B) Staining of healthy and reactive BM with antibody against PD-1 is generally negative with a rare lymphocyte showing membranous staining. (C) Strong staining of placental syncytiotrophoblasts is shown with antibody against PD-L1. (D) Staining of tonsil with antibody against PD-1 highlights a subset of T cells in the germinal center, as shown at right. Magnification $\times 40$ in panels A,C-D and $\times 100$ in panel B. Images taken with an Olympus BX41 microscope with Olympus cellSens standard version 1.14 software, and standard color balancing and image sizing using Adobe Photoshop.

evaluate the univariate association between each covariate and PD-1/PD-L1 expression. $P < .05$ was considered statistically significant.

Results

IHC analysis reveals increased PD-L1 in mastocytosis

To define the distribution of PD-L1 and PD-1 in neoplastic cells in mastocytosis and other myeloid neoplasms (of AHN type), we performed IHC on tissues from a range of mastocytosis subtypes (Table 2) and compared this with expression in a variety of neoplastic and nonneoplastic BM conditions (Table 3). We found that PD-L1-expressing cells are increased in number in SM and CM (Figure 1), whereas no increase was observed in other myeloid neoplasms tested, including MPNs, MDSs, and MDS/MPNs (typical AHN-type disorders). An increase in PD-1⁺ and/or PD-L1⁺ cells was also not seen in MMAS or in healthy and reactive BMs (Table 3; Figure 2). In the advanced SM cases examined, we found expression of PD-L1 in all patients with MCL and ASM, and in 75% of patients with SM-AHN. In each case, checkpoint antigen expression was confirmed to be confined to the SM component only by comparison with tryptase, CD117, and CD25 IHC. Expression, when present, appeared to be restricted to MCs and was not identified in lymphocytes or other cell types. Expression of PD-L1 was also seen in the MCs of a single case of MML. With respect to smoldering SM and ISM, PD-L1 expression was found in neoplastic cells in 1 of 2 patients (50%) and 3 of 4 patients (75%), respectively. Irrespective of the subtype of SM, there appears to be a correlation between the intensity of staining with PD-L1 and the percentage of PD-L1 MCs (supplemental Figure 1). Additionally, we found PD-L1 expression in the majority of CM cases (23 of 25, 92%), which included all mastocytomas and all “mastocytosis in skin” (MIS) lesions from patients with systemic disease, with a high percentage of maculopapular CM (MPCM) also being positive (15 of 17, 88%). PD-L1 staining of MCs in individual cases was membranous and ranged from 10% to 100% (mean, 50%) with

57% of cases showing dim and 43% of cases showing strong staining intensity.

Neoplastic MCs display cell-surface PD-L1 by flow cytometry

As assessed by multicolor flow cytometry, primary MCs obtained from patients with ISM or advanced SM were found to express PD-L1 but did not express detectable PD-1 on their cell surface (Figure 3A-B), supporting the IHC observations in the previous paragraph. The MCL-like cell lines HMC-1.1 and HMC-1.2 were found to express low levels of PD-L1 and PD-1 (Figure 3C). These data demonstrate that PD-L1 is expressed on the surface of neoplastic MCs in SM, independent of the WHO type of the disease.

Multiplex IHF reveals a heterogeneous expression of PD-L1 in MCL

To better characterize the coexpression of PD-L1 expression on MCs, we used multiplex IHF to simultaneously visualize tryptase-positive MCs and PD-L1⁺ cells. We first examined tissue from 1 of the 3 patients with MCL (patient 1; Figures 4 and 5). Although tryptase-positive and PD-L1⁺ cells were both found in the spleen of this patient with MCL, only a subset of MCs coexpressed PD-L1, particularly those present at the edge of the infiltrate (Figure 4). Many of the PD-L1⁺ cells were found to be tryptase negative, indicating that the majority of these cells are not MCs, and may represent tumor-infiltrating immune cells or resident splenic macrophages. During imaging, we noted that MCs often cluster around the periarteriolar lymphatic sheaths (PALS). To further examine this spatial distribution, we used laser-scanning confocal microscopy to acquire images from multiple regions of interest that were then stitched together to visualize a larger area in the spleen while retaining high resolution. Figure 6 demonstrates that PD-L1⁺ MCs are often located close to the PALS and their frequency decreases with further distance from the PALS.

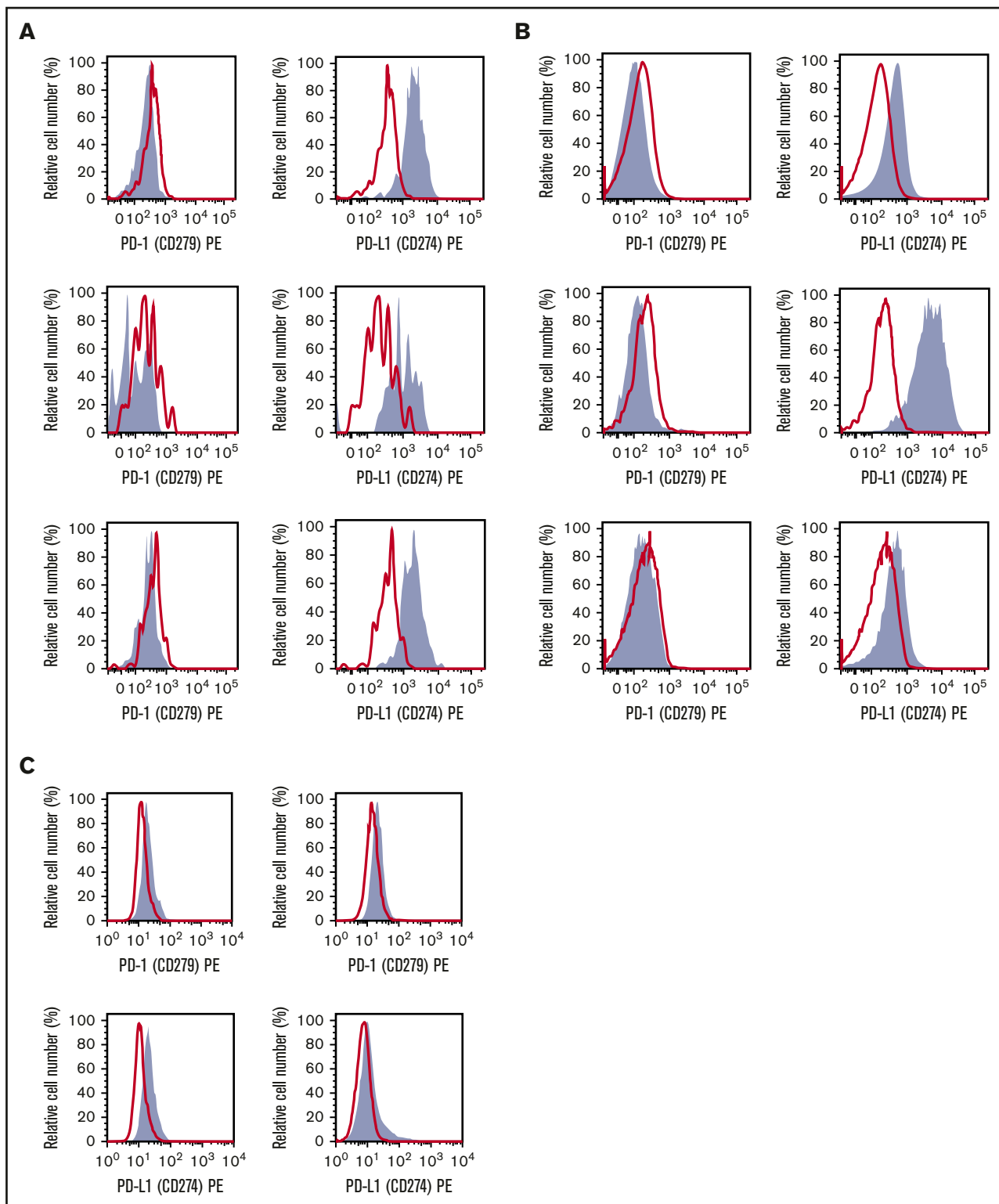


Figure 3. Expression of PD-L1 on the surface of neoplastic MCs in SM. (A-B) $KIT^+/CD34^-$ BM MCs obtained from 3 patients with ISM (A) and 3 with advanced SM (2 with MCL, 1 with ASM) (B) were stained with antibodies against PD-1 (CD279) (left subpanels) or PD-L1 (CD274) (right subpanels) by multicolor flow cytometry as described in "Materials and methods." Antibody staining is shown in gray. The isotype-matched control is also shown (red lines and open histograms). (C) The MCL-derived human MC lines HMC-1.1 ($KIT\ D816V^-$) (left subpanel) and HMC-1.2 ($KIT\ D816V^+$) (right subpanel) were stained with antibodies against PD-1 (top subpanels) or PD-L1 (bottom subpanels).

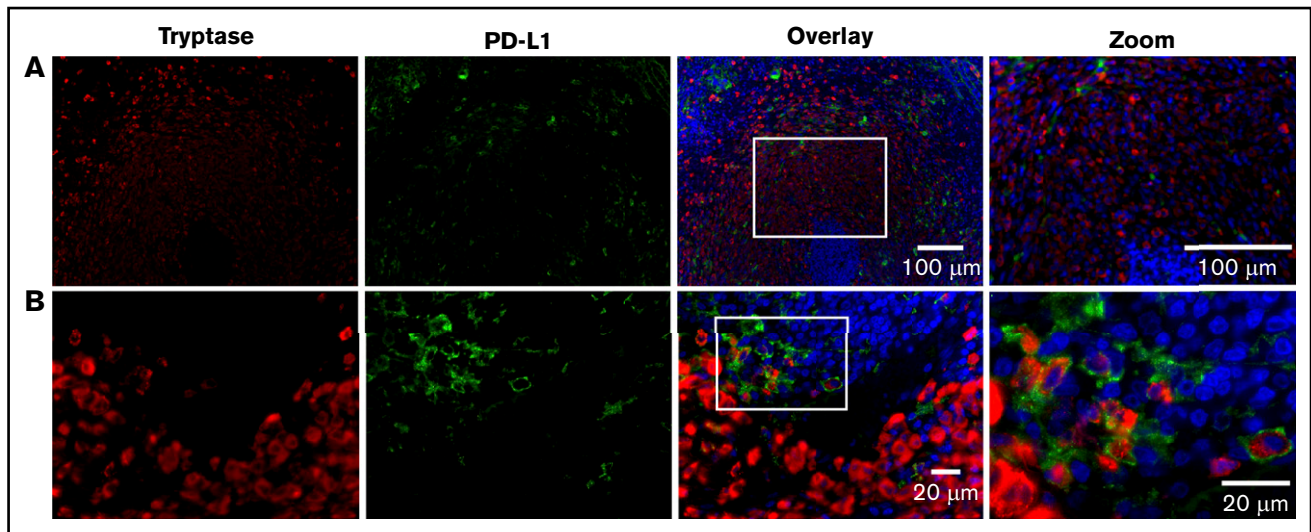


Figure 4. Expression of PD-L1 occurs on MCs in MCL. Splenic tissue from a patient with MCL was stained for MCs (tryptase, red), PD-L1 (light green), and nuclei (DAPI, blue). (A) Image acquired at $\times 20$ magnification. Scale bars, 100 μm . Note the MC nest localized around the PALS. (B) Image acquired at $\times 63$ magnification. Scale bars, 20 μm . White boxes in overlay image denote the region magnified in the right column. The coexpression of PD-L1 and tryptase in MCs is demonstrated at high power, however, only a subset of MCs is positive for PD-L1. Smaller numbers of PD-L1⁺ cells lacking tryptase coexpression are also seen at the edge of MC infiltrates.

Higher frequency of expression of PD-L1 in CM

PD-L1 expression was observed in 92% of the cases with CM by IHC (Tables 2 and 3). A uniform pattern of membrane expression of PD-L1 was seen in neoplastic MCs of CM (Figure 1) by IHC across different cases. We examined 1 case of CM with IHF for PD-L1 to assess the heterogeneity of expression by MCs. In comparison to MCL, we found a higher frequency of PD-L1 and tryptase coexpressing MCs in the CM tissue in these cases (Figure 7).

PD-1 expression is restricted to CM

PD-1 showed dim membranous staining in neoplastic MCs in 4 of 27 CM cases (15%) using IHC. Staining was found in a higher percentage of mastocytomas (67%) compared with MPCM (11%), and was not found in any skin lesions from patients with SM (0 of 6). PD-1 expression was not observed in other mastocytosis subtypes, in other neoplasms tested, or in reactive and healthy BMs (Table 3; Figures 1 and 2). PD-1 staining of MCs ranged from 20% to 50% (mean, 27%). Expression, when present, was restricted to MCs and was not identified in lymphocytes or other cell types. In healthy BM, a rare lymphocyte was noted to be PD-1⁺ (Figure 2).

Discussion

PD-1 is an immune checkpoint receptor expressed on activated T cells and a small subset of B cells in germinal centers, whereas PD-L1 is expressed on activated T cells, dendritic cells, monocytes, and tumor cells from a variety of malignancies. PD-1 is known to interact with its ligands, PD-L1 and PD-L2, to protect tissues from immune-mediated damage and this interaction between PD-1 and PD-L1 also allows neoplastic cells to evade immune destruction. Recent work has shown PD-L1 expression on a variety of tumor cells, including melanoma, renal cell carcinoma, lung carcinoma, head and neck carcinomas, gastrointestinal malignancies, bladder carcinoma, ovarian carcinoma, and Hodgkin lymphoma cells.¹⁰ In

2015, Rabenhorst and investigators showed that serum levels of soluble PD-L1 correlated with disease severity in 31 adult patients with SM and further documented in a few patients expression of PD-L1 in BM and skin biopsies of patients with SM, with expression of PD-1 in skin biopsies only.⁷ In 2016, Kuklinski and Kim described strong diffuse PD-L1 immunohistochemical expression in skin biopsies from 12 patients with mastocytosis.¹¹ The patients were a mix of pediatric and adult patients, including 5 possible patients with SM, but the authors did not use the WHO 2016 classification to uniformly categorize patients. Thus, it is unclear what subtypes of SM were present. The results from our systematic evaluation of a larger number of patients with mastocytosis support these findings, documenting PD-L1 expression in 77% of BM biopsies, including both ISM and advanced SM, and in 92% of skin biopsies. Other MPNs, MDSs, reactive and healthy BMs did not show expression of PD-1 or PD-L1 in MCs. Flow cytometric studies confirm the expression of PD-L1 on the surface of neoplastic MCs. We further explored the variability of expression of PD-L1 using IHF and showed variability of expression of PD-L1 within the architecture of tumor samples, albeit in a limited number of samples. This is intriguing, as PD-L1 expression in other tumors, such as melanoma, shows a variable pattern of PD-L1 expression focused primarily at the interface between melanocytes and infiltrating immune cells.¹² This difference in expression of PD-L1 in mastocytosis is also important as the “positivity” of PD-L1 varies significantly from patient to patient and may impact selection of candidates for, and response to, anti-PD-L1 therapy.¹³ However, expression of PD-L1 in melanoma shows only partial correlation with response to anti-PD-L1 treatment. Thus, our findings suggest that anti-PD-L1 therapy might be a promising option in patients with advanced mastocytosis, although the expression of PD-L1 does not necessarily predict response to such treatment.

In the SM and CM samples examined, only the neoplastic MCs expressed PD-L1 in BM and skin biopsies, respectively. Other immune cell types, including lymphocytes, did not express PD-L1 in these tissue types. In splenic tissue, smaller numbers of immune

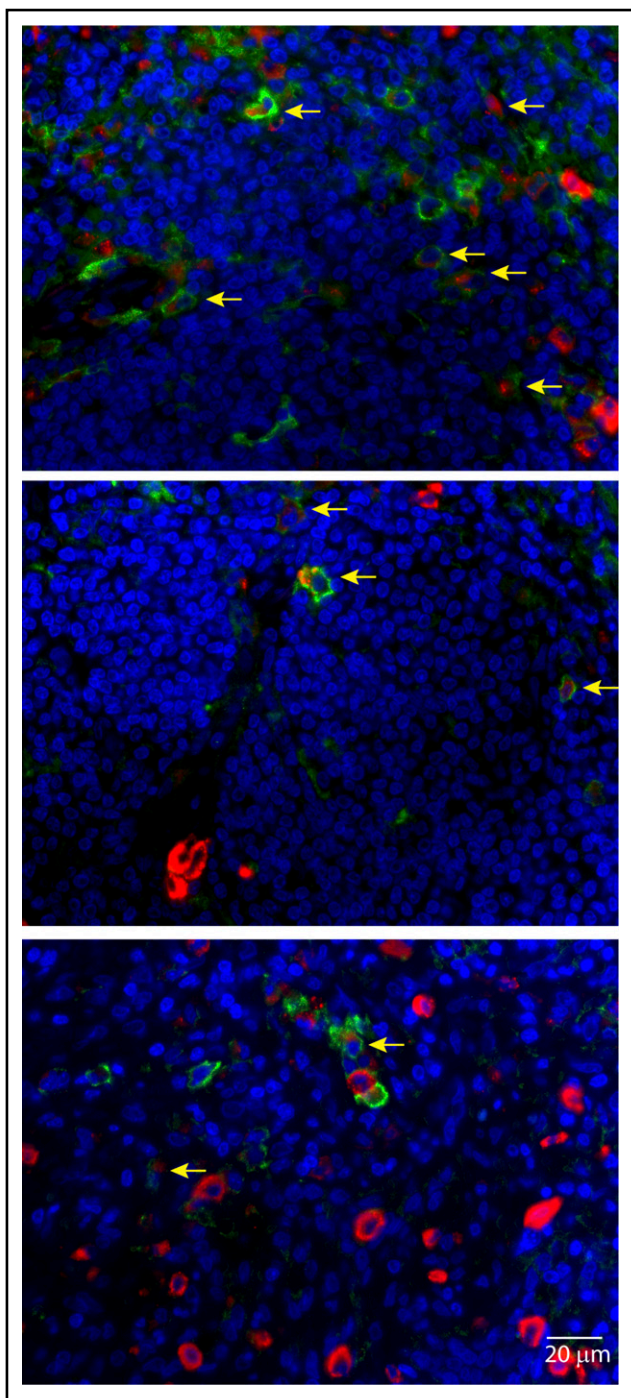


Figure 5. Further examples of tryptase (red) and PD-L1 (light green) coexpression on MCs in spleen from a MCL patient. Cell nuclei are blue (DAPI). Images acquired at 60 \times magnification. Scale bar, 20 μ m. Coexpression is indicated by yellow arrows. A subset of MCs lacking PD-L1 expression is noted. Small numbers of PD-L1⁺ cells lacking tryptase expression are also present.

cells did express PD-L1, primarily at the edge of MC infiltrates, and these were favored to be lymphocytes based on morphology. Expression of PD-1 was noted in 15% of the CM samples examined, and in all samples tested, PD-1 expression was seen in MCs exclusively. Again, admixed immune cells such as

lymphocytes did not express PD-1 in either SM or CM samples. This is intriguing because tumor responses with anti-PD-1/PD-L1 immunotherapy are mediated by tumor antigen-specific T cells.^{14,15} Both innate and adaptive models have been described in different tumor types to explain PD-L1 expression.¹⁶ Some, but not all, samples with mastocytosis have reactive T-cell infiltrates, including CD8⁺ T cells. Those mastocytosis samples with T-cell infiltrates may have inducible PD-L1 expression at the site of the T-cell infiltrate (an adaptive pattern), which would support a more variable staining pattern than we observed in PD-L1 expression in SM. In mastocytosis without T-cell infiltrates, one can argue that the positive PD-L1 expression is likely regulated by genetic or epigenetic events intrinsic to the neoplastic MCs (ie, constitutive PD-L1 expression), rather than reactive to a T-cell response. Several different genetic mechanisms have been reported to lead to this latter innate pattern including gene amplification, loss of tumor suppressor genes, or oncogenic driver mutations, resulting in overexpression of PD-L1 on all neoplastic cells.¹³ Rabenhorst et al showed that in fact there is more soluble PD-L1 in the supernatant of *KIT* D816V-mutant HMC-1 and ROSA cells.⁷ The PD-L1 positivity in the presence or absence of a T-cell infiltrate may predict response to immunotherapy, with the presence of T cells predicting a positive response. Given the differences in T-cell infiltrates by organ type in mastocytosis, one could also speculate whether immunotherapy would be effective in all sites of disease.

With respect to PD-1 expression in CM, our findings confirm the previous literature that only a subset of patients with CM expresses PD-1.¹⁷ In 2013, Kataoka and colleagues published the first report of PD-1 expression in CM, confirmed with reverse transcription–polymerase chain reaction, western blotting, and flow cytometry. They documented that 10 of 30 cases of CM expressed PD-1.¹⁷ The patients with CM were not subclassified as to type, but the widespread ages that are given suggest a mix of CM and SM patients, where the latter had likely MIS lesions. Thus, we cannot easily separate whether the CM patients that expressed PD-1 were in fact only CM patients. In the Rabenhorst manuscript, a single patient with CM was included for IHC staining with PD-1.⁷ In our study, there is negativity of PD-1 staining in all MIS skin biopsies, whereas 11% of MPCM and 67% of mastocytomas show dim, but uniform, staining with PD-1. These results suggest that the expression of PD-1 by neoplastic MCs in CM is not driven by the microenvironment, but rather is intrinsic to these MCs due to factors unknown at this point.

Our study indicates that there may be a complex cancer-immune interaction occurring between MCs in disease and regulatory immune cells. More studies should be undertaken to determine the nature and extent of this interaction, further correlation with *KIT* mutation status, serum tryptase levels, and CD25 expression, as well as the expression levels on healthy and neoplastic MCs to further extend our understanding of the pathophysiology of MC disease. This would be an important step to determine what implications PD-1 and PD-L1 expression may have for rational drug design in advanced mastocytosis.

Acknowledgments

The authors thank Genevieve Phillips for assistance with confocal imaging.

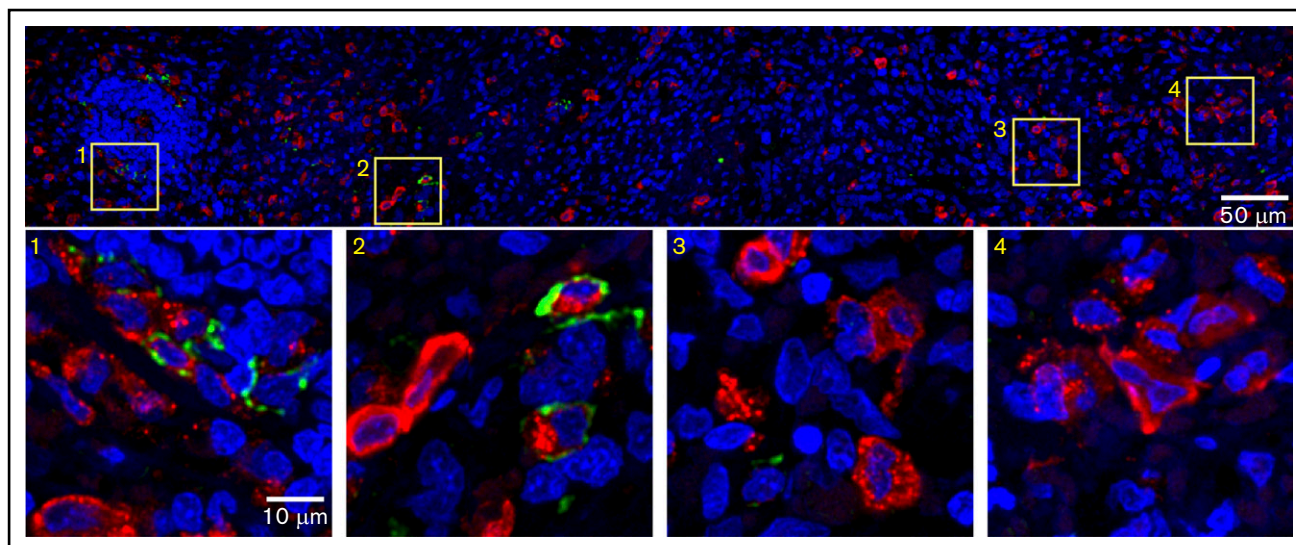


Figure 6. PD-L1-coexpressing MCs aggregate near the PALS structure in MCL. Splenic tissue was stained for expression of tryptase (red), PD-L1 (light green), and nuclei (DAPI, blue). (Top panel) Seven regions of interest acquired by confocal microscopy were stitched together to provide a larger field of view. Images are the maximum projection of 3 z-sections. Total field of view is 184.52 µm × 1290.24 µm; scale bar, 50 µm. (1-4) Magnification of corresponding boxes in top panel. Scale bar, 10 µm. Note that PD-L1⁺ MCs are more frequently found near the PALS.

This work was supported by grants from the National Institutes of Health, National Institute of General Medical Sciences (R01GM100114 [D.S.L.] and P50GM085273 [New Mexico Spatiotemporal Modeling Center]) and National Institute of Diabetes

and Digestive and Kidney Diseases (K01DK097206) (H.H.W.); the University of New Mexico, Department of Pathology (T.I.G.); and the German Research Council (HA 2393/6-1) (K.H.). P.V. was supported by the Austrian Science Fund (FWF), grant SFB F4704-B20. Fluorescence images in this paper were generated in the University of New Mexico and Cancer Center Fluorescence Microscopy Shared Resource (National Cancer Institute grant 2P30 CA118100). Statistics were performed in the University of New Mexico Comprehensive Cancer Center Biostatistics Shared Resource.

Authorship

Contribution: T.I.G., D.S.L., and K.H. conceived the idea for the study, with T.I.G. designing the IHC experiments, D.S.L. and H.H.W. the IHF experiments, and P.V. the flow cytometry experiments; J.G. and P.V. provided patient samples; IHC data were collected by M.E.S. and T.I.G., with analysis by M.B.G. and T.I.G., and figure preparations by D.S.L. and T.I.G.; IHF data collection was performed by E.W.H., C.M., and H.H.W., with analysis and figure preparation by E.W.H., C.M., D.S.L., and H.H.W.; flow cytometry data were collected by G.E. and K.B., with analysis and figure preparation by P.V., G.E., and K.B.; statistics were performed by J.-H.L. and L.C.; the manuscript was written by M.B.G., E.W.H., P.V., D.S.L., and T.I.G.; and all authors reviewed the manuscript and gave critical input.

Conflict-of-interest disclosure: T.I.G. and D.S.L. received research funding from Allakos. T.I.G. and J.G. received consulting fees from Blueprint Medicine. T.I.G., P.V., J.G., and K.H. received consulting fees from Novartis and were on a midostaurin trial study steering committee for Novartis. K.H. received consulting fees from ALK and Deciphera. P.V. received research grants from Deciphera and Blueprint. P.V. and K.H. received a research grant from Novartis. The remaining authors declare no competing financial interests.

The current affiliation for C.M. is Oregon Health Sciences University, Portland, OR.

The current affiliation for T.I.G. is Department of Pathology, University of Utah, Salt Lake City, UT.

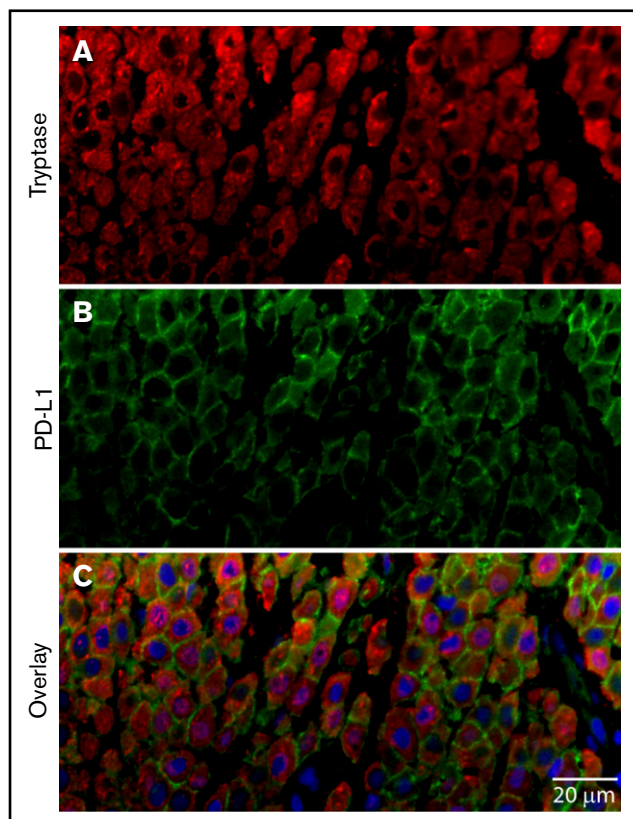


Figure 7. PD-L1⁺ MCs in CM. Skin biopsy from a patient with CM was stained for expression of (A) tryptase (red), (B) PD-L1 (light green), and (C) nuclei (DAPI, blue). Scale bar, 20 µm. The majority of MCs show PD-L1 membrane labeling.

ORCID profiles: M.E.S., 0000-0001-6696-0061; K.H., 0000-0002-4595-8226; P.V., 0000-0003-0456-5095; H.H.W., 0000-0002-8502-3679; D.S.L., 0000-0001-8533-6029; T.I.G., 0000-0001-5478-7847.

Correspondence: Tracy I. George, Department of Pathology, University of Utah School of Medicine, 500 Chipeta Way, Salt Lake City, UT 87108; e-mail: tracy.george@path.utah.edu.

REFERENCES

1. George TI, Sotlar K, Valent P, Horny H-P. Mastocytosis. In: Jaffe ES, Arber DA, Harris NL, eds. Hematopathology. 2nd ed. Philadelphia, PA: Elsevier; 2017:911-930.
2. Valent P, Horny HP, Escribano L, et al. Diagnostic criteria and classification of mastocytosis: a consensus proposal. *Leuk Res*. 2001;25(7):603-625.
3. Nagata H, Worobec AS, Oh CK, et al. Identification of a point mutation in the catalytic domain of the protooncogene c-kit in peripheral blood mononuclear cells of patients who have mastocytosis with an associated hematologic disorder. *Proc Natl Acad Sci USA*. 1995;92(23):10560-10564.
4. Ustun C, Arock M, Kluin-Nelemans HC, et al. Advanced systemic mastocytosis: from molecular and genetic progress to clinical practice. *Haematologica*. 2016;101(10):1133-1143.
5. Ostrand-Rosenberg S, Horn LA, Haile ST. The programmed death-1 immune-suppressive pathway: barrier to antitumor immunity. *J Immunol*. 2014;193(8):3835-3841.
6. Topalian SL, Drake CG, Pardoll DM. Targeting the PD-1/B7-H1 (PD-L1) pathway to activate anti-tumor immunity. *Curr Opin Immunol*. 2012;24(2):207-212.
7. Rabenhorst A, Leja S, Schwaab J, et al. Expression of programmed cell death ligand-1 in mastocytosis correlates with disease severity. *J Allergy Clin Immunol*. 2016;137(1):314-318.
8. Valent P, Sotlar K, Sperr WR, et al. Refined diagnostic criteria and classification of mast cell leukemia (MCL) and myelomastocytic leukemia (MML): a consensus proposal. *Ann Oncol*. 2014;25(9):1691-1700.
9. Valent P, Akin C, Metcalfe DD. Mastocytosis: 2016 updated WHO classification and novel emerging treatment concepts. *Blood*. 2017;129(11):1420-1427.
10. Swaika A, Hammond WA, Joseph RW. Current state of anti-PD-L1 and anti-PD-1 agents in cancer therapy. *Mol Immunol*. 2015;67(2 Pt A):4-17.
11. Kuklinski LF, Kim J. Expression of PD-L1 in mastocytosis. *J Am Acad Dermatol*. 2016;74(5):1010-1012.
12. Taube JM, Anders RA, Young GD, et al. Colocalization of inflammatory response with B7-h1 expression in human melanocytic lesions supports an adaptive resistance mechanism of immune escape. *Sci Transl Med*. 2012;4(127):127ra37.
13. Ribas A, Hu-Lieskovan S. What does PD-L1 positive or negative mean? *J Exp Med*. 2016;213(13):2835-2840.
14. Pardoll DM. The blockade of immune checkpoints in cancer immunotherapy. *Nat Rev Cancer*. 2012;12(4):252-264.
15. Tumeh PC, Harview CL, Yearley JH, et al. PD-1 blockade induces responses by inhibiting adaptive immune resistance. *Nature*. 2014;515(7528):568-571.
16. Berry S, Taube JM. Innate vs. adaptive: PD-L1-mediated immune resistance by melanoma. *Oncol Immunology*. 2015;4(10):e1029704.
17. Kataoka TR, Fujimoto M, Moriyoshi K, et al. PD-1 regulates the growth of human mastocytosis cells. *Allergol Int*. 2013;62(1):99-104.